

Analytical model of transit time broadening for two-photon excitation in a three-level ladder and its experimental validation

M. Bruvelis,^{*} J. Ulmanis,[†] N. N. Bezuglov,[‡] K. Miculis, C. Andreeva,[§] B. Mahrov, D. Tretyakov,^{||} and A. Ekers
Laser Centre, University of Latvia, LV-1002 Riga, Latvia

(Received 23 March 2012; published 6 July 2012)

We revisit transit time broadening for one of the typical experiment designs in molecular spectroscopy, that of a collimated supersonic beam of particles crossing a focused Gaussian laser beam. In particular, we consider a Doppler-free arrangement of a collimated supersonic beam of Na₂ molecules crossing two counterpropagating laser beams that excite a two-photon transition in a three-level ladder scheme. We propose an analytical two-level model with a virtual intermediate level to show that the excitation line shape is described by a Voigt profile and provide the validity range of this model with respect to significant experimental parameters. The model also shows that line broadening due to the curvature of laser field wave fronts on the particle beam path is exactly compensated by increased transit time of particles farther away from the beam axis, such that the broadening is determined solely by the size of the laser beam waist. The analytical model is validated by comparing it with numerical simulations of density-matrix equations of motion using a split propagation technique and with experimental results.

DOI: [10.1103/PhysRevA.86.012501](https://doi.org/10.1103/PhysRevA.86.012501)

PACS number(s): 33.70.Jg, 32.70.Jz, 31.15.—p

I. INTRODUCTION

The limited interaction time of atoms or molecules with the exciting laser field is well known to affect resolution in a variety of spectroscopy applications, including Doppler-free two-photon spectroscopy [1–7], saturated absorption spectroscopy [8–13], photon echo spectroscopy [14,15], precise determination of the optical frequency [16–18], heterodyne molecular spectroscopy [19,20], and others. Here, we consider the spectral line broadening caused by finite transit time τ_{tr} of particles through a laser beam, which is a typical concern for atomic and molecular beam experiments. The transit time broadening is further affected by the finite width of the velocity distribution of particles in the beam, which leads to an effective distribution of transit times. Given a sufficiently short transit time, the measured linewidths in the excitation or absorption spectra become notably larger than the natural linewidths of optical transitions.

One can distinguish between two qualitatively different situations depending on how the transit time τ_{tr} compares to the natural lifetime τ_{sp} of the excited level. If $\tau_{tr} \gg \tau_{sp}$, the line broadening can take place due to nonstationary effects, such as velocity-selective optical pumping [4,7,11], depletion broadening in the weak excitation limit [21], or transit time relaxation [22–24]. Transit time effects in this long interaction time limit have been well described in the above-cited studies; therefore we shall not address them in this paper. If τ_{tr} becomes comparable to (or smaller than) τ_{sp} , the

transit time notably affects the observed spectral linewidths [25,26]. Intuitively, this broadening can be understood from Heisenberg’s uncertainty principle (in what follows atomic units are used): $\Delta\tau\Delta\varepsilon \sim 1$. Uncertainty of energy $\Delta\varepsilon$ of an excited state is affected not only by its spontaneous lifetime ($\Delta\tau \approx \tau_{sp}$) but also by the transit time ($\Delta\tau \approx \tau_{tr}$). Hence, a decreased transit time will lead to an increased uncertainty of energy, which will manifest itself in a spectroscopic measurement as line broadening.

A semiquantitative representation of the broadened linewidth can be obtained using a simple model, which assumes adiabatical switching of the laser-atom interaction. Let us consider the equations of motion for density matrix ρ in the general case of a quantum system of n levels [27,28]:

$$\frac{d\rho}{dt} = -i[H, \rho] - \frac{1}{2}(\Gamma\rho + \rho\Gamma) + L(\rho). \quad (1)$$

The Hamiltonian H describes the “atom plus laser field” system, the diagonal matrix $\Gamma_{ij} = \Gamma_i\delta_{ij}$ describes the spontaneous emission with decay constants $\Gamma_i = 1/\tau_{sp}^{(i)}$, and $L(\rho)$ describes the cascade effects. Note that for an open system $L(\rho) = 0$. In the rotating-wave approximation (RWA) and under the bare states representation [29] Eq. (1) can be reduced to a steady-state form by averaging both sides of the equation over the light-atom interaction time T , $\langle \dots \rangle = T^{-1} \int_0^T dt \dots$, and assuming $\rho(T) \approx \langle \rho \rangle$ with $\langle [H_{st}, \rho] \rangle \approx [\langle H_{st} \rangle, \langle \rho \rangle]$:

$$\frac{\rho(0)}{T} = \frac{\langle \rho \rangle}{T} + i[\langle H_{st} \rangle, \langle \rho \rangle] + \frac{1}{2}(\Gamma \langle \rho \rangle + \langle \rho \rangle \Gamma) - L(\langle \rho \rangle), \quad (2)$$

where H_{st} is the bare states representation of the Hamiltonian H . For the diagonal matrix $\hat{T}_{ij} = \delta_{ij}/T$ it is convenient to rewrite the term $\langle \rho \rangle / T$ as $(\hat{T}\rho + \rho\hat{T})/2$ and incorporate it in the spontaneous emission terms. Formally, it corresponds to redefining all decay constants as $\Gamma_i \rightarrow \tilde{\Gamma}_i = \Gamma_i + 1/T$ (including the ground state). Normally, atoms would enter the laser field in their ground state $i = 0$; hence the initial density matrix is $\rho_{ij}(0) = \delta_{i0}$. Note that the additional decay

^{*}martins.bruvelis@lu.lv

[†]Present address: Physikalisches Institut, Ruprecht-Karls-Universität Heidelberg, 69120 Heidelberg, Germany.

[‡]Permanent address: Faculty of Physics, St. Petersburg State University, 198904 St. Petersburg, Russia.

[§]Permanent address: Institute of Electronics, BAS, 1784 Sofia, Bulgaria.

^{||}Permanent address: Institute of Semiconductor Physics, SB RAS, 630090 Novosibirsk, Russia.

terms $1/T$ in $\tilde{\Gamma}_i$ are partly compensated due to the generation of new atoms by the source function on the left-hand side of Eq. (2); for a closed system the latter ensures that the total population in all levels i is preserved [22,23].

For a two-level atom, the Hamiltonian $\langle H_{st} \rangle$ and the cascade term $L(\langle \rho \rangle)$ are

$$\begin{aligned} \langle H_{st} \rangle &= \begin{bmatrix} -\Delta & \langle \Omega \rangle / 2 \\ \langle \Omega \rangle / 2 & 0 \end{bmatrix}, \\ L(\langle \rho \rangle) &= \begin{bmatrix} 0 & 0 \\ 0 & \Lambda_{br} \Gamma_1 \langle \rho \rangle_{11} \end{bmatrix}, \end{aligned} \quad (3)$$

where Δ is the detuning of laser frequency off from resonance, $\langle \Omega \rangle$ is the average Rabi frequency, and Λ_{br} is the branching ratio, i.e., the part of the spontaneous decay going from the upper level 1 to the lower level 0. In the limiting case of an open system $\Lambda_{br} = 1$, while for a closed system $\Lambda_{br} = 0$. In the weak excitation limit (i.e., when $\langle \rho \rangle_{11} \ll \langle \rho \rangle_{00}$) the solution of Eq. (2) yields the excitation spectrum $P(\Delta) = \Gamma_1 T \langle \rho \rangle_{11}$ (see details in Sec. III A), which is described by the well-known Lorentz function [6,28]:

$$\begin{aligned} P(\Delta) &= \frac{\Gamma_1}{1/T + \Gamma_1} \frac{\tilde{\Gamma} \langle \Omega \rangle^2}{4\Delta^2 + \Delta\omega_L^2}, \\ \Delta\omega_L &= \tilde{\Gamma} = \tilde{\Gamma}_0 + \tilde{\Gamma}_1 = \Gamma_1 + 2/T, \end{aligned} \quad (4)$$

where $\Delta\omega_L$ is the full width at half maximum (FWHM). It remains to be clarified how parameter T relates to the transit time τ_{tr} . Intuitively, it would be straightforward to assume $T = \tau_{tr}$, which corresponds to the uncertainty relation $\tau_{tr} \Delta\varepsilon \sim \Lambda$ with $\Lambda = 2$. However, quantum-mechanics manuals state that the value of Λ is strongly dependent on the pulse shape of the coupling light field.

In the present study we consider an effective two-level system passing through a relatively weak laser beam with a Gaussian intensity distribution. Specifically, we measure experimentally (Sec. II) and analyze theoretically (Sec. III) line shapes $P(\Delta)$ in the laser-excitation spectra of Na_2 molecules in a supersonic beam. The weak excitation limit allows us to study “pure” transit time effects, ignoring a range of other mechanisms, such as power broadening, formation of dark states, interference within a system of laser-dressed states, etc., which arise when laser intensities are close to (or larger than) the saturation limit and a proper theoretical treatment of which involves complicated mathematics [9]. Using the approach developed in [30], we shall derive an analytical expression for $P(\Delta)$ for an arbitrary ratio between τ_{tr} and τ_{sp} and show that it takes the form of Voigt’s profile.

Under the conditions of our experiment there are two competitive processes that contribute to the formation of line profiles. This is illustrated in Fig. 1. Tight focusing of the laser beam ensures short transit times of molecules through the laser beam waist of size w_0 , which are well below the natural lifetime of the excited state and lead to a significant line broadening. However, the wave-front radius $R(z)$ of the tightly focused laser beam rapidly changes along the laser beam axis z on both sides of the focus, such that in all planes other than the xy plane at $z = 0$ the wave fronts are curved [6]. The molecules crossing the laser beam near $z \sim 0$ experience shorter transit times and hence larger transit time broadening

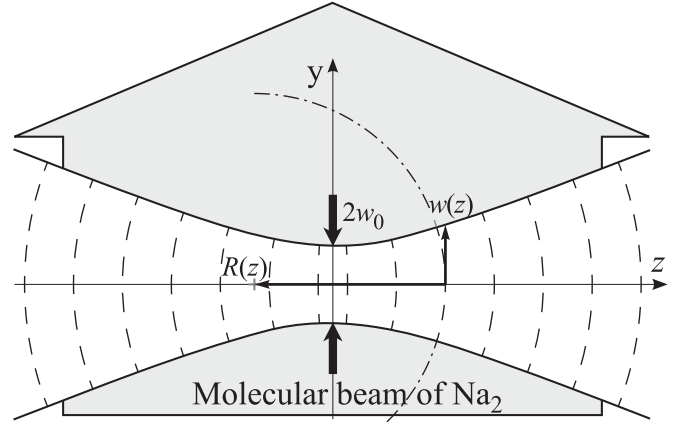


FIG. 1. A laser field with a Gaussian intensity distribution described by Eqs. (5) and (6) propagates along the z axis. It is focused by a cylindrical lens with the focal plane at $z = 0$ and a beam waist w_0 , and it crosses the molecular beam propagating along the y axis. Molecules moving at distances $|z| > 0$ experience longer interaction times with the laser field and hence exhibit a smaller transit time broadening compared to molecules moving at $z = 0$. At the same time, the molecules moving at $|z| > 0$ are crossing curved wave fronts of the light field; hence they experience phase shifts of the light field along their trajectories, which introduce additional line broadening [6]. The dash-dotted line demonstrates the curvature of a wave front with radius $R(z)$ at distance z from the Gaussian beam waist, which corresponds to a beam width $w(z)$.

than the molecules crossing the laser beam farther away from the focal plane. At the same time, the molecules crossing the laser beam farther away from the focal plane experience additional broadening due to phase shifts introduced by the curved wave fronts. In Sec. III we shall demonstrate that both competing broadening mechanisms cancel each other exactly, such that the width of the spectral line does not change along the z axis and is determined solely by the transit time of molecules through the beam waist $\tau_{\min} = 2w_0/v_f$, where v_f is the flow velocity of molecules in the supersonic beam.

One-photon excitation line shapes are affected by a small but finite residual Doppler broadening even in well-collimated supersonic beams [21,31]. In our supersonic beam the residual FWHM Doppler width for excitation at right angles to the beam axis at a wavelength of 633 nm is $\Delta v_{\text{Dop}} \sim 25$ MHz, which is not acceptable for the intended studies of transit time broadening. We therefore implement a two-photon excitation scheme with counterpropagating laser beams, whereby the excitation spectrum is measured by fixing the frequency of one of the laser fields at a certain detuning off from one-photon resonance while scanning the frequency of the other laser field across the two-photon resonance. The two-photon excitation is realized in a three-level ladder system of Na_2 (see Fig. 2). The first laser field P couples the populated rovibrational level g in the ground electronic state with the intermediate level e in the $A^1\Sigma_u^+$ state with Rabi frequency Ω_P . The second laser field S couples the intermediate level e with the final level f in the $5^1\Sigma_g^+$ state with Rabi frequency Ω_S . In Sec. III we shall demonstrate that such an arrangement allows us to describe the excitation of level f in terms of interaction of a two-level system with a single effective laser field with Rabi frequency

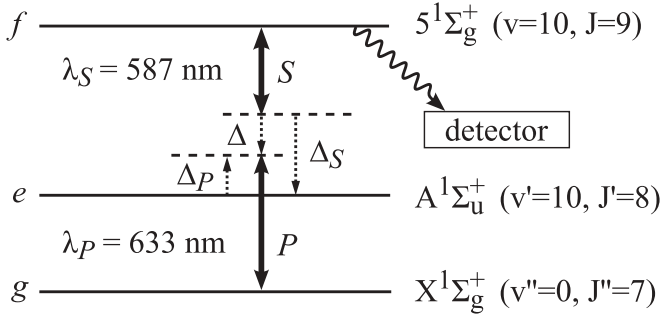


FIG. 2. Three-level ladder scheme in Na_2 . The S laser field with $\lambda_S = 587$ nm couples levels e and f and is detuned off from the one-photon resonance by Δ_S . Levels g and e are coupled by the P laser field with $\lambda_P = 633$ nm, which is scanned across the two-photon resonance at $\Delta_P = -\Delta_S$. The measured total fluorescence from level f as a function of $\Delta = \Delta_P + \Delta_S$ represents the excitation spectrum of the two-photon transition.

$\Omega_{\text{eff}} \simeq \Omega_P \Omega_S / (2|\Delta_S|)$. In order to fully simulate a two-level system, we exclude direct population of the intermediate level e by detuning the P laser field by $|\Delta_P| \approx |\Delta_S| \gg \Gamma_e$, such that level e is converted into a virtual level. The excitation spectrum of level f is then obtained as a function of two-photon detuning Δ . In Sec. IV we shall demonstrate that theoretical predictions obtained in such a way are in good agreement with the experiment.

II. EXPERIMENT

The experiment was performed in a collimated supersonic beam of Na_2 molecules with a mean flow velocity $v_f = 1340$ m/s and the full $1/e$ width of the velocity distribution $\Delta v = 260$ m/s. Two skimmers and a 2.3-mm-diameter entrance aperture of the excitation chamber collimate the beam to the divergence angle of $0.73^\circ \pm 0.02^\circ$, which corresponds to the residual FWHM Doppler widths of 25 and 27 MHz for the one-photon excitation wavelengths of 633 and 587 nm, respectively. The number density of molecules in the laser excitation zone was estimated from the known vapor pressure inside the beam source and the geometry of the beam apparatus as $\approx 2 \times 10^{10}$ cm $^{-3}$ using the formulas provided in [32] and knowing that for the beam operation parameters as in the current experiment the fraction of molecules in the beam is about 1/10 [33]. Supersonic expansion cools the molecules such that 99% of them are in the ground vibrational level $v'' = 0$ of the $X^1\Sigma_g^+$ state, while the distribution over the rotational levels peaks at $J'' = 7$ with about 8.6% of the population in this level. With these numbers and using the formulas provided in [34] for the specific case of radiation trapping in collimated beams, it is easy to demonstrate that the mean number of photon scattering events for photons within the $X^1\Sigma_g^+ \rightarrow A^1\Sigma_u^+$ absorption band is $\bar{N} < 1.002$, and hence any contribution to line broadening due to radiation trapping can be safely disregarded.

The molecular beam was crossed by two counterpropagating laser beams at right angles. Both laser beams were from Coherent CR-699-21 ring dye lasers with linewidths of 1 MHz. The P laser beam ($\lambda = 633$ nm) and the S laser beam ($\lambda = 587$ nm) were obtained by operating the dye lasers

with [2-[2-[4-(dimethylamino)phenyl]ethenyl]-6-methyl-4H-pyran-4-ylidene]-propanedinitrile (DCM) and Rh6G dyes, respectively. Wavelengths of both laser fields were measured to an accuracy of ± 0.0001 nm using the High Finesse WS/7 Wavemeter. The laser beams were transmitted to the excitation chamber using single-mode polarization maintaining optical fibers, sent through polarizers, and focused onto the molecular beam using cylindrical lenses, such that the long axis of the focus was perpendicular to the molecular beam axis with the $1/e^2$ width of the beam along the x axis of ≈ 1 cm. The waists $2w_0$ of the P and S laser beams along the z axis were measured by the THORLABS Optical Slit Beam Profiler BP104-VIS as (26.1 ± 0.5) and (86 ± 0.5) μm , respectively, and their linear polarizations were set parallel to the molecular beam axis. The effective transit time of molecules through the more tightly focused P laser beam was $\tau_{tr} = 2w_0/v_f = 19$ ns. For comparison, natural lifetimes of the levels e and f are $\tau_e = 12.45$ ns [35] and $\tau_f = 35$ ns [36], respectively. The counterpropagating arrangement of laser beams reduced the effective Doppler broadening for two-photon excitation to about 1 MHz.

The P and S laser fields with frequencies ω_P and ω_S , respectively, coupled the ladder of three Na_2 rovibrational levels, g , e , and f , as illustrated in Fig. 2. The frequency of the S laser field was detuned off from the e - f resonance frequency ω_{fe} by $\Delta_S = \omega_S - \omega_{fe}$. The frequency of the P laser field was scanned across the two-photon resonance g - f while monitoring the total fluorescence emitted from level f as a function of two-photon detuning Δ . The latter relates to one-photon detunings as $\Delta = \Delta_P + \Delta_S$, where $\Delta_P = \omega_P - \omega_{eg}$ is the one-photon detuning of the P laser field from the e - g resonance frequency ω_{eg} . The two-photon excitation spectra were recorded for various fixed detunings Δ_S and various intensities of the P and S laser fields.

The fluorescence emitted by molecules in level f and in the electronic state $A^1\Sigma_u^+$ state was collected by two lenses and imaged onto a fiber bundle and a multimode fiber. Light transmitted by the fiber bundle was sent through a cutoff filter transmitting light with $\lambda < 600$ nm; the transmitted fluorescence originates from transitions from level f to a number of rovibrational levels in the $A^1\Sigma_u^+$ state. This light was further sent to a photomultiplier, and the resulting signal was registered by a photon counter as a function of two-photon detuning Δ . The fluorescence detected in this way is hereafter referred to as the two-photon excitation spectra $P(\Delta)$. The fluorescence transmitted by the single-mode fiber was registered by the Ocean Optics SD2000 fiber-optics spectrometer, and it allowed the monitoring of vibration-resolved emission spectra from the $A^1\Sigma_u^+$ and $5^1\Sigma_g^+$ states. Together with accurate laser wavelength measurements, the vibration-resolved spectra served as a reference for the identification of laser-excited levels.

A. Experimental results

Figure 3 shows two-photon excitation spectra $P(\Delta)$ of level f at different detunings Δ_S of the S laser field. Rabi frequencies were determined using the Autler-Townes effect [37,38], and they were found to be 63 and 100 MHz for P -field and S -field coupling, respectively. The effective Rabi frequencies

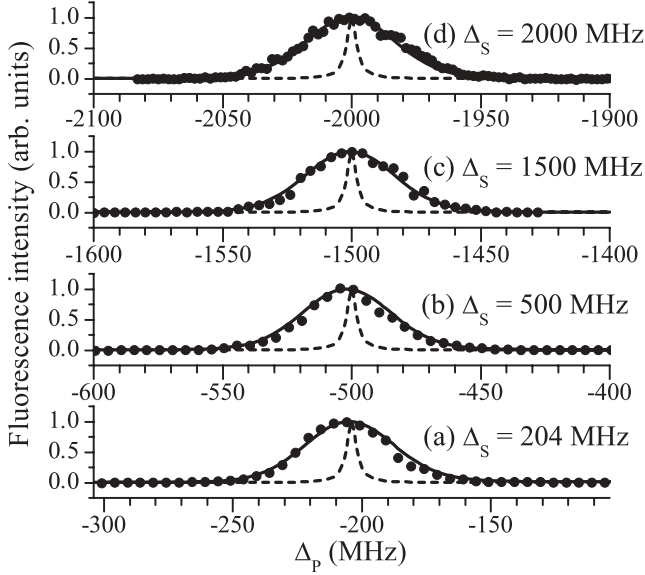


FIG. 3. Excitation spectra of level f for different detunings Δ_S of the S laser field. Note that the P laser detuning Δ_P differs from the two-photon detuning $\Delta = \Delta_P + \Delta_S$ at fixed Δ_S . Dots are the experimental data points, while solid lines show the results of numerical simulations described in Sec. III. Signals are normalized to the intensity maximum. For comparison, the dashed line shows the expected natural linewidth.

$\Omega_{\text{eff}} \simeq \Omega_P \Omega_S / (2|\Delta_S|)$ corresponding to the four detunings of Δ_S in Fig. 3 are summarized in Table I. The experimental profiles appear to be significantly broader than the natural linewidth (see dashed line in Fig. 3), indicating that substantial transit time broadening takes place. These measured spectra will be compared with the results of numerical simulations and discussed in more detail in Sec. IV.

III. THEORETICAL LINE PROFILES

Given a sufficiently large detuning of S and P laser fields from the respective one-photon resonances, level e is virtual, and it can be disregarded in the Schrödinger equation and the density-matrix equations of motion describing the dynamics of the three-level system g - e - f . Such a step is justified by the adiabatic elimination principle [29], when the amplitude c_e of the virtual level can be exactly expressed via the remaining two levels. In the following section we shall consider the two-level case, while potential effects of the virtual level will be analyzed in Sec. III B.

A. Analysis of a two-level system

Consider two-level particles with ground state g and excited state f propagating in the molecular beam along the y axis

TABLE I. Effective Rabi frequencies Ω_{eff} of the two-photon transition for different detunings Δ_S (all values in MHz).

	Δ_S			
	204	500	1500	2000
$ \Omega_{\text{eff}} $	15.7	6.3	2.1	1.6

with flow velocity v_f , as depicted in Fig. 1. The laser beam with wavelength $\lambda_L = 2\pi/k_L$ propagates along the z axis. The particles cross the Gaussian laser beam of frequency ω_L , which is focused by a cylindrical lens to a beam waist w_0 (see Fig. 1). Along the x axis the laser intensity varies only by 5% across the particle beam diameter; hence it is justified to consider it as constant in this direction. Along the y and z axes the electric-field amplitude E has the following spatial distribution:

$$\begin{aligned}
 E &= \text{Re}A(y,z)E_0 \exp(-i\omega_L t + ik_L z), \\
 A(y,z) &= \exp\{-i[\varphi(z) + (k_L/2q)y^2]\}, \\
 \varphi(z) &= \frac{1}{2} \left[\arctan\left(\frac{\lambda_L z}{\pi w_0^2}\right) - i \ln \sqrt{1 + \frac{\lambda_L z}{\pi w_0^2}} \right], \\
 q &= i\pi w_0^2/\lambda_L + z.
 \end{aligned} \tag{5}$$

Equations (5) can be easily obtained using the methods described in [39] for the case of focusing by a spherical lens. The amplitude E depends on the slowly varying complex function $A(z,y)$, and it does not depend on the x coordinate due to focusing by the cylindrical lens. Note that the phase $\varphi(z)$ entering Eqs. (5) is two times smaller than in the original expression [6,39] for spherical lenses.

In order to get a better impression about the shape of the electric-field amplitude E it is helpful to insert parameter q into the expression for $A(z,y)$ [6]:

$$\begin{aligned}
 A(z,y) &= \exp\left(-\frac{y^2}{w^2(z)}\right) \exp\left[-i\frac{k_L y^2}{2R(z)} - i\varphi(z)\right], \\
 w^2(z) &= w_0^2 \left[1 + (\lambda_L z/\pi w_0^2)^2\right], \\
 R(z) &= z \left[1 + (\pi w_0^2/\lambda_L z)^2\right].
 \end{aligned} \tag{6}$$

Then Eq. (6) describes a Gaussian beam with z -dependent width $w(z)$ and a y -dependent phase, which is in turn determined by the z -dependent wave-front curvature $R(z)$. For a particle crossing the laser beam at coordinate z such a distribution results in Gaussian switching of Rabi frequency:

$$\Omega_z(t) = \Omega_0 A(tv_f, z), \tag{7}$$

where $\Omega_0 = E_0 \langle f|d_z|g \rangle$ is the Rabi frequency of the g - f coupling in the center ($z = 0$) of the laser beam that is linearly polarized along the y axis. Importantly, particles traveling in the y direction at various distances z from the molecular beam axis experience different interaction times with the laser field due to the variation of laser beam size $w(z)$. As we shall demonstrate, this latter circumstance does not affect the excitation spectra.

A qualitative interpretation of the observed two-photon excitation spectra $P(\Delta)$ can be obtained by using the Schrödinger equation in RWA and bare states representation for an open system without cascade transitions [28,38]:

$$\frac{d}{dt}c_f = -i(\Delta - i\Gamma_f/2)c_f - i\Omega_z(t)/2c_g, \tag{8}$$

$$\frac{d}{dt}c_g = -i\Omega_z^*(t)/2c_f,$$

$$J_z = \Gamma_f \int_{-\infty}^{\infty} dt |c_f(t)|^2, \tag{9}$$

where zero energy corresponds to the energy of level g , the decay rate $\Gamma_f = 1/\tau_{\text{nat}}$ determines the natural width of level f , and Δ is the detuning of the laser frequency. The integral J_z gives the probability for a particle traveling at distance z to emit a photon; i.e., it describes the excitation spectrum of a single particle.

Initially, a particle entering the excitation zone is in level g , which sets the boundary conditions for the amplitudes of levels g and f as $c_f(-\infty) = 0$ and $c_g(-\infty) = 1$. Following [30], we assume that the weak excitation limit implies a negligible depletion of the ground state and set $c_g \simeq 1$ at all times, thus obtaining from Eqs. (8) an explicit time dependence of $c_f(t)$. The latter determines the induced electric dipole moment $\mathbf{d}_+(t) = \langle f_i | \mathbf{d} | g_t \rangle = c_f^*(t) \langle f | \mathbf{d} | g \rangle$ and allows us to find the observable fluorescence signal J_z after performing the Fourier transform $\tilde{c}_f(\omega')$ of the amplitude $c_f(t)$:

$$J_z = \int_{-\infty}^{\infty} d\omega' I_z(\omega'), \quad I_z(\omega') = \Gamma_f |\tilde{c}_f(\omega')|^2 / 2\pi. \quad (10)$$

In order to find $\tilde{c}_f(\omega')$, it is convenient to rewrite Eqs. (8) in the Fourier space:

$$i\omega \tilde{c}_f(\omega') = i(\Delta - i\Gamma_f/2)\tilde{c}_f(\omega') - i\tilde{\Omega}_z(\omega')/2, \quad (11)$$

$$\tilde{\Omega}_z(\omega') = \Omega_0 \sqrt{\frac{2\pi q}{ik_L v_f^2}} \exp\left(-i\varphi(z) + \frac{iq\omega'^2}{2k_L v_f^2}\right). \quad (12)$$

Equation (12) gives an explicit representation of the Fourier transform of Rabi frequency $\Omega_z(t)$ (7) for the Gaussian function $A(z, tv_f)$, Eq. (5). Equation (11) immediately yields

$$I_z(\omega') = \Gamma_f \frac{|\tilde{c}_f(\omega')|^2}{2\pi} = \frac{1}{2\pi} \left(\frac{\Gamma_f |\tilde{\Omega}_z(\omega')|^2}{4(\omega' - \Delta)^2 + \Gamma_f^2} \right). \quad (13)$$

Since the equations are written in RWA, the reference point of frequency ω' is the laser frequency: $\omega' = \omega - \omega_L$. Inserting the $\tilde{\Omega}_z$ expression (12) into (13), we obtain $I_z(\omega')$ for the case of excitation by a Gaussian laser beam:

$$I_z(\omega') = \frac{w_0^2}{2v_f^2} \sqrt{\frac{1 + \frac{4z^2}{w_0^4 k_L^2} \Gamma_f \Omega_0^2 \exp\left(-\frac{w_0^2 \omega'^2}{2v_f^2}\right)}{1 + \frac{2z}{w_0^2 k_L} \frac{4(\omega' - \Delta)^2 + \Gamma_f^2}{\Gamma_f^2}}}. \quad (14)$$

The excitation spectrum $P(\Delta)$ of an individual particle at coordinate z is identical to the probability J_z [Eq. (9)], and it is obtained by integrating $I_z(\omega')$ over frequencies ω' [see Eq. (10)]. The integration yields a Voigt profile resulting from the convolution between Gaussian and Lorentz functions [40]:

$$P_z(\Delta) = \frac{\tau_{tr}^2 \Gamma_f \Omega_0^2}{8} \sqrt{\frac{1 + \frac{4z^2}{w_0^4 k_L^2}}{1 + \frac{2z}{w_0^2 k_L} \frac{\Gamma_f^2}{\Gamma_f^2 + 4(\omega - \Delta)^2}}} \int_{-\infty}^{\infty} \frac{d\omega \exp\left(-\frac{\tau_{tr}^2 \omega^2}{8}\right)}{\Gamma_f^2 + 4(\omega - \Delta)^2}, \quad (15)$$

where $\tau_{tr} = 2w_0/v_f$. Importantly, coordinate z does not enter the integral determining the dependence of P_z on Δ . Hence, all particles have identical excitation spectra regardless of the distance z from the beam waist at which they cross the laser beam; the only parameter varying with z is the amplitude factor, which determines how many molecules at a given z contribute to the total signal. The result represented by Eq. (15) is significant: the line shape does not depend on z . This

surprising result can be interpreted in terms of transit time *and* phase shift broadening. An increase in z results in larger phase shifts along the trajectory of a traversing molecule and also larger transit times. While the broadening due to the phase shift increases, the broadening that arises from larger transit times decreases, leading to broadening that is independent of z .

Note that according to our definition $\tau_{tr} = 2w_0/v_f$ the transit time corresponds to the time interval needed for a molecule traveling along $z = 0$ to traverse the full width at e^{-2} of the spatial laser intensity distribution. Hence, the function $P_z(\Delta)$ is associated with the central trajectory of particles ($z = 0$).

In the limiting case of a very short transit time $\tau_{tr} \ll \tau_{\text{nat}} = 1/\Gamma_f$ the excitation spectrum given by Eq. (15) reduces to a Gaussian profile $P_z(\Delta) \sim \exp(-\tau_{tr}^2 \Delta^2/8)$, which coincides with the textbook result described in [6]. The corresponding FWHM is $\Delta\omega_G = 4\sqrt{\ln 4}/\tau_{tr}$. The other limiting case of a very large transit time $\tau_{tr} \gg \tau_{\text{nat}}$ results in the Lorentz profile with FWHM determined solely by the natural broadening: $\Delta\omega_{\text{Lor}} = \Gamma_f$. For all intermediate cases the FWHM of the Voigt profile (15) can be accurately (within an error bar better than 0.02%) approximated by the expression given in [41]:

$$\Delta\omega_V = 0.5346\Gamma_f + \sqrt{0.2166\Gamma_f^2 + 22.18/\tau_{tr}^2}. \quad (16)$$

Our derivation of Eq. (15) is valid in the weak excitation limit, when only a small fraction of population is pumped out of the ground state during the interaction with the laser field. For an open system it means that the probability for an atom in the upper level to emit a photon, which is described by $P(\Delta)$, is equal to the probability of ground-state depletion. Hence, the result (15) is valid if $P_{z=R_b}(0) \ll 1$ for molecules experiencing the longest interaction time with a resonant laser field at $z = R_b$, where R_b is the molecular beam radius ($R_b = 1.15$ mm in our experiment). Using the estimates of the Voigt profile provided in [41], the probability can be simplified to

$$P_{z=R_b}(0) \simeq \frac{\pi \tau_{tr}^2 \Omega_0^2}{2(8 + \sqrt{2\pi} \tau_{tr} \Gamma_f)} \sqrt{1 + \frac{2R_b}{w_0^2 k_L}} \ll 1. \quad (17)$$

Equation (17) has a clear physical meaning. If Γ_f is disregarded, the equality $\tau_{tr} \Omega_0 = \pi$ corresponds to the realization of a π pulse. Inequality (17) is equivalent to the requirement of insufficient laser power for realization of population inversion.

Note that mechanisms of the formation of Voigt profile $P(\Delta)$, Eq. (15), in the case of collimated beams and in the case of thermal gases are different. In the former case all molecules have nearly the same velocity v_f , and the Voigt profile results from Gaussian switching of coupling between the molecules and the laser field, while in the latter case it results from the Maxwell velocity distribution of the absorbing and emitting molecules.

B. Effect of the intermediate level

When the intermediate level e is treated as virtual, care should be taken to properly take into account constraints on all relevant parameters of the three-level system. Even a weak coupling of both laser fields with level e results in dynamical Stark shifts of the other two levels, g and f [42,43]. Such shifts

TABLE II. Constraints for applicability of the effective two-level model. Row (5*) is not mandatory and is need for the optional requirement $|C_e| < |C_f|$.

N	Parameters	Restrictions
(1)	Δ_P, Δ_S	$ \Delta_P , \Delta_S \ll \omega_P, \omega_S, \omega_P - \omega_S $
(2)	Δ_P, Δ_S	$ \Delta_P , \Delta_S \gg \Gamma_e, \Gamma_f$
(3)	Δ_P, Δ_S	$\tau_{ir} \Delta_P \gg 1; \tau_{ir} \Delta_S \gg 1$
(4)	Δ_P, Δ_S	$ \Delta = \Delta_P + \Delta_S \ll \Delta_P , \Delta_S $
(5*)	Ω_S	$ \Omega_S > 2 \Delta $
(6)	$\tilde{\Gamma}_g$	$ \Omega_P ^2 \Gamma_e \tau_{ir} \ll 4\Delta_P^2$
(7)	$\Delta \varepsilon_i$	$\Omega_P \approx \Omega_S$
(8)	$\Delta \varepsilon_i$	$\tau_{ir}^{(S)} \approx \tau_{ir}^{(P)}$
(9)	Ω_{eff}	$ \Omega_{\text{eff}} \ll \max\{1/\tau_{ir}, \Gamma_f\}$

may noticeably broaden the spectral profile of the effective two-photon transition $g \rightarrow f$. For level e to be validly treated as virtual, a number of conditions have to be satisfied, as summarized in Table II.

Strictly speaking, the line shape $P(\Delta)$ should be considered either in the framework of density-matrix formalism [27] or using the Floquet theory [44,45]. However, since both approaches involve relatively complicated treatment, we shall rely instead on the more transparent analysis of the Schrödinger equation in RWA for an open system [38].

The constraints of Table II can be interpreted as follows. Row (1) represents the validity conditions of RWA, which are discussed in detail in [45]; it requires that there should be no interplay between couplings by both laser fields: each laser excites only one relevant transition and not the other one.

To prevent levels g and f from sharing their population with level e , the one-photon detunings of the P and S laser fields should be kept sufficiently large [row (2) of Table II] [42]. This allows one to disregard the presence of the decay constants Γ_i ($i = g, f$) when they are combined with the detunings Δ_i . Choosing the energy of bare state e as $\varepsilon_e = 0$, the energies of bare states g and f become $\varepsilon_g = \Delta_P$ and $\varepsilon_f = -\Delta_S$, respectively (see Fig. 2); the two-photon detuning is expressed as $\Delta = \varepsilon_g - \varepsilon_f = \Delta_P + \Delta_S$.

The population of level e is associated with the excitation of electric dipole oscillators of g - e and e - f with the decay constants $\Gamma_{ei} = (\Gamma_i + \Gamma_e)/2$ ($i = g, f$). If the oscillator excitation times $\tau_{ei} \simeq 1/\sqrt{\Gamma_{ei}^2 + \Delta_i^2} \simeq 1/|\Delta_i|$ are much smaller than the transit time, i.e., when [see row (3) of Table II]

$$\tau_{ir}|\Delta_i| \gg 1, \quad \varepsilon_g = \Delta_P, \quad \varepsilon_f = -\Delta_S, \quad (18)$$

then the amplitude $C_e(t)$ of level e immediately adjusts to the amplitudes $C_i(t) = \tilde{C}_i(t) \exp(-i\varepsilon_i t)$, whereby $\tilde{C}_i(t)$ is a comparatively slowly varying function of time. The procedure of adiabatic elimination of $C_e(t)$ yields [28,29]

$$C_e(t) = \frac{\Omega_P(t)}{2\varepsilon_g} C_g(t) + \frac{\Omega_S^*(t)}{2\varepsilon_f} C_f(t). \quad (19)$$

After insertion of the expression for C_e into the Schrödinger equation the three-level problem reduces to an effective two-

level form:

$$\begin{aligned} \frac{d}{dt} C_f &= -i \left(\varepsilon_f - i \frac{\Gamma_f}{2} + \frac{|\Omega_S|^2}{4\varepsilon_f} \right) C_f - i \frac{\Omega_S \Omega_P}{4\varepsilon_g} C_g, \\ \frac{d}{dt} C_g &= -i \left(\varepsilon_g + \frac{|\Omega_P|^2}{4\varepsilon_g} \right) C_g - i \frac{\Omega_P^* \Omega_S^*}{4\varepsilon_f} C_f. \end{aligned} \quad (20)$$

Here, the nondiagonal elements $\tilde{\Omega}_{f,g} = \Omega_S \Omega_P / 4\varepsilon_g$ and $\tilde{\Omega}_{g,f} = \Omega_P^* \Omega_S^* / 4\varepsilon_f$ correspond to the effective two-level Rabi frequencies $\Omega_{\text{eff}}/2$ [cf. Eqs. (8)]. Usually, these elements should be self-conjugated ($\tilde{\Omega}_{g,f} = \tilde{\Omega}_{f,g}^*$), and it is possible to meet this requirement by imposing the restriction presented in row (4) of Table II for the two-photon detuning Δ . Under such conditions $\varepsilon_g \simeq \varepsilon_f$ and Ω_{eff} becomes (see also in [46])

$$\Omega_{\text{eff}} \simeq \frac{\Omega_S \Omega_P}{2\Delta_P} \simeq -\frac{\Omega_S \Omega_P}{2\Delta_S}. \quad (21)$$

In general, Eqs. (20) are not self-conjugated, which is due to the fact that level e is slightly excited and thus not fully virtual. This excitation channels a small fraction of the population out of the effective two-level system g - f , leading to nonconservation of the total population $|C_g|^2 + |C_f|^2$. The situation changes when two-photon resonance is realized at $\varepsilon_g = \varepsilon_f$ (i.e., $\Delta_P = -\Delta_S$): a stable dark state consisting exclusively of levels g and f is formed [28,42,47], which prevents the population flow to level e , which thus restores the self-conjugation of Eqs. (20).

For the intermediate level to be treated as virtual it is necessary to ascertain that the population $|C_e|^2$ of level e is negligible. For this purpose it is comfortable to use the well-known estimate of the amplitude $|C_e| \sim |\Omega_P|/|2\Delta_P|$ [28] and compare it with the amplitude $|C_f| \sim |\Omega_{\text{eff}}|/|2\Delta|$. Taking into account the expression for Ω_{eff} (21), the requirement $|C_e| < |C_f|$ results in an additional constraint on the experimental parameters given in row (5*) of Table II. Note, however, that such a requirement is not mandatory for the validity of Eqs. (20); hence row (5*) is optional.

IV. RESULTS AND DISCUSSION

In the solution of Eqs. (20) care should be taken due to the presence of the terms

$$\Delta \varepsilon_f = \frac{|\Omega_S|^2}{4\varepsilon_f}, \quad \Delta \varepsilon_g = \frac{|\Omega_P|^2}{4\varepsilon_g}, \quad (22)$$

which have the physical meaning of dynamic Stark shifts due to coupling with the intermediate level e and can strongly modify the energies of bare states g and f with respect to the initial two-photon detuning. These energy shifts are also associated with the so-called reactive effects in atom-light interaction [42]. The interaction introduces additional loss of population from levels g and f due to sharing their population with level e , and the decay constants should be accordingly modified to account for this effect [42]:

$$\tilde{\Gamma}_f = \Gamma_f + \frac{|\Omega_S|^2}{4\Delta_P^2 + \Gamma_e^2} \Gamma_e, \quad \tilde{\Gamma}_g = \frac{|\Omega_P|^2}{4\Delta_S^2 + \Gamma_e^2} \Gamma_e. \quad (23)$$

In Eqs. (20) the additional terms entering Γ_i (associated with the so-called dissipative effects) have been ignored since,

according to row (2) of Table II, we have disregarded them compared to energy shifts $\Delta\varepsilon_i$ (22).

A. Other constraints of the two-level model

In realistic experiments one can seldom isolate a closed three-level system; open three-level systems prevail. In order to avoid depletion and power broadening in the excitation spectrum of level f , one should therefore ensure that all parameters describing the interaction of this system with laser fields fulfill a number of additional requirements that are summarized in rows (6)–(9) of Table II. Row (6) corresponds to $\tilde{\Gamma}_g \tau_{ir} \ll 1$ and implies that depletion of the ground state is negligible [21]. We assume that both laser beams are Gaussian, Eq. (6), such that molecules experience Gaussian switching of Rabi frequencies:

$$\begin{aligned}\Omega_z^{(P)}(t) &= \Omega_P A_P(z, tv_f), \\ \Omega_z^{(S)}(t) &= \Omega_S A_S(z, tv_f).\end{aligned}\quad (24)$$

During the interaction with laser fields the energy level shifts $\Delta\varepsilon_i(t)$ ($i = g, f$) are time dependent, and they follow the switching of Rabi frequencies $\Omega_z^{(P,S)}(t)$. The two-photon detuning $\Delta(t) = \Delta + \Delta\varepsilon_g - \Delta\varepsilon_f$ is swept around its initial value $\Delta = \varepsilon_g - \varepsilon_f$, effectively leading to a blurred two-photon resonance. There are two scenarios how this can be avoided: (i) by using equal Rabi frequencies and equal durations of both laser pulses [rows (7) and (8) in Table II] or (ii) by keeping the values of Rabi frequencies Ω_P and Ω_S close while limiting the value of Ω_{eff} [row (9) in Table II]. The first approach ensures that $\Delta\varepsilon_f(t) \simeq \Delta\varepsilon_g(t)$ and $\Delta(t) \simeq \Delta$ at all times. The second approach makes use of the fact that Ω_{eff} is well below the saturation limit and meets the requirement of Eq. (17); since $|\Delta\varepsilon_i(t)| \sim \Omega_{\text{eff}}$, the amplitude of sweep of the two-photon detuning $\Delta\varepsilon_f(t) - \Delta\varepsilon_g(t)$ is much smaller than the characteristic linewidth ($\sim \max\{1/\tau_{ir}, \Gamma_f\}$), such that it cannot notably affect the two-level excitation profile (15).

In practice it may be nontrivial to precisely realize scenario (i) by satisfying the requirements of rows (7) and (8) of Table II. Moreover, in the beginning and at the end of laser-molecule interaction, when both Rabi frequencies $\Omega_z^{(P,S)}(t)$ are small, the constraint of row (5*) is not valid. In order to ensure that $|C_e| < |C_f|$, we have chosen the interaction time of molecules with the S laser field much larger than the interaction time with the P laser field, $\tau_{ir}^{(S)} \gg \tau_{ir}^{(P)}$. In experiment this is easily achieved by increasing the waist of the S laser beam. Such an arrangement ensures that by the time when the coupling of molecules with the P laser field becomes noticeable the value of $\Omega_z^{(S)}(t)$ is already close to its maximum. In our experiment the transit times through the S and P laser fields are $\tau_{ir}^{(S)} = 63$ ns and $\tau_{ir}^{(P)} = 19$ ns, respectively. Since the amplitude of the S laser field is nearly constant at times when the P laser pulse evolves, we can assume $A_S(z, tv_f) \simeq 1$ for the relevant time scale. This means that the effective Rabi frequency

$$\Omega_z^{(\text{eff})}(t) = \Omega_{\text{eff}} A_P(z, tv_f) A_S(z, tv_f) \quad (25)$$

follows essentially the amplitude of the P laser pulse $A_S(z, tv_f)$. For our experiment this means that transit time with respect to the effective Rabi frequency $\Omega_z^{(\text{eff})}(t)$ corresponds to 19 ns.

B. Numerical simulation of the full sublevel system

In some experimental situations it may be difficult to fulfill the requirements of Table II, and the two-level model may be inapplicable. In that case numerical calculations of the dynamics involving the full level and sublevel system are required. In our earlier study [36] we described a computational scheme that allows one to perform such exact numerical modeling for the level system shown in Fig. 2 taking into account the full Zeeman sublevel structure and possible cascade effects. Following that scheme, we employ the split propagation technique [48,49] to solve numerically the density-matrix equations (1). From the known molecular transition moments [50,51] we estimate that about 5% of the population returns from level e to level g and about 30% returns from level f to level e via spontaneous emission. The observed fluorescence signal S_f from level f is proportional to the integrated over time total population of level f :

$$S_f \sim \sum_{m_J} \int_{-\infty}^{\infty} dt \rho_{m_J, m_J}^f(t). \quad (26)$$

We assume that initially all Zeeman sublevels of the lower level g are equally populated and no coherences are present. The dependence of the Rabi frequency on the magnetic quantum number m_J is given by Clebsch-Gordan coefficients. Both laser fields are linearly polarized in the same direction parallel to the molecular beam axis, implying the selection rule $\Delta m_J = 0$ for the quantization axis chosen parallel to the directions of laser polarizations. Rabi frequencies for each ladder consisting of three m_J sublevels are obtained from the mean Rabi frequencies (24) as

$$\begin{aligned}\Omega_P(m_J) &= \frac{1.061}{8} \sqrt{8^2 - m_J^2} \Omega_z^{(P)}(t), \\ \Omega_S(m_J) &= \frac{1}{9} \sqrt{9^2 - m_J^2} \Omega_z^{(S)}(t).\end{aligned}\quad (27)$$

Although we use excitation by counterpropagating laser beams leading to the cancellation of Doppler broadening, we still perform averaging over the thermal velocity distribution of molecules along the molecular beam axis in order to account for the spread of transit times for molecules of different velocity groups.

C. Comparison between analytical and numerical results

When the constraints of Table II are met in the experiment, the intermediate level e is to a good approximation virtual and one can expect the two-level formulas (see in Sec. III A) to properly describe the observed excitation spectrum. Since the waist of the P laser beam (13 μm) is essentially smaller than that of the S laser beam (43 μm), the profile of the space (time) dependence of the effective Rabi frequency $\Omega_z^{(\text{eff})}$, Eq. (25), coincides with that of $\Omega_z^{(P)}(t)$, Eq. (24).

Figure 4 shows a comparison between the analytical two-level result described by the Voigt profile (15) and the full numerical simulation: neither profile is distinguishable in the scale of the figure. Such agreement justifies our reasoning that molecules traveling at different coordinates z with respect to the particle beam axis exhibit essentially identical excitation profiles despite the fact that the size $w(z = 1.15 \text{ mm})$ of

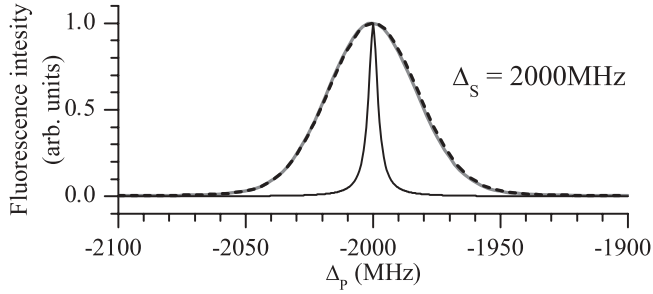


FIG. 4. Comparison of different line broadening models for detuning $\Delta_S = 2000$ MHz as in Fig. 3: the gray solid line is the result of accurate numerical simulations for the level system of Fig. 2 taking into account the full magnetic sublevel structure; the dashed line corresponds to the two-level Voigt profile (15); the solid black line is the Lorentz profile that takes into account only the natural broadening of level f .

the P laser beam at the outer edge of the molecular beam is twice the beam waist $w(z=0)$. The width of both the numerical and analytical profiles is in a good agreement with the FWHM value $\Delta\nu_V = 42$ MHz obtained from the approximate formula (16). For comparison, natural broadening due to the spontaneous decay of level f leads to the FWHM Lorentz width of $\Delta\nu_{\text{nat}} = 4.5$ MHz.

D. Comparison with experiment

Figures 3 and 4 show that both the analytical two-level model and the full numerical simulation appropriately describe the observed excitation spectra: in the scale of the figure the theoretical line profiles are indistinguishable from each other. The coincidence of both theoretical results is due to the fact that level e is virtual for the chosen range S field detunings [Table II, rows (1)–(4)] and the Rabi frequencies $\Omega_{P,S}$ and Ω_{eff} satisfy the weak excitation conditions [Tables I and II, rows (5), (6), and (9)]. Hence, the two-level model is a good approximation, and the Voigt profile (15) is practically equal to the numerical one (see Fig. 4).

For Rabi frequencies $\Omega_P(m_j)$ and $\Omega_S(m_j)$ as in the present experiment, a notable disagreement with the two-level model can be expected for $|\Delta_S| < \Delta\nu_V = 42$ MHz, when the non-negligible population of level e occurs due to transit time broadening. At such detunings one-photon transitions become

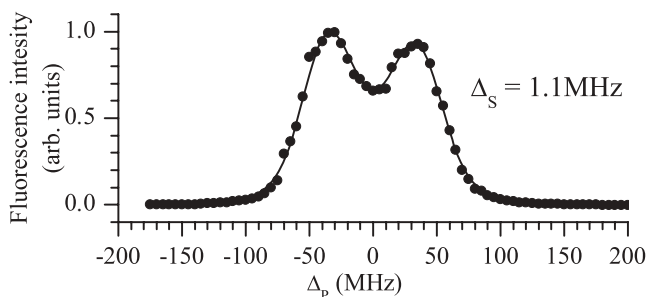


FIG. 5. The excitation profile for the final f state in the case of small S laser detuning. The solid line exhibits numerical results, while dots corresponds to experimental data.

relevant, and a full numerical simulation must be performed. Figure 5 shows an example of the excitation profile when $|\Delta_S|$ is smaller than the transit time broadening. The two peaks of the profile correspond to the Autler-Townes doublet [37,38], each component of which relates to the excitation of one of the two dressed states resulting from coupling of level e with level f due to interaction with the S laser field. However, even in this case of comparatively strong coupling, the transit time effect appears to dominate in the line broadening, and FWHM widths of both peaks is about 44 MHz.

V. CONCLUSIONS

We have analyzed the effects of limited transit time on line broadening in the excitation spectra for a typical experimental situation of a beam of particles crossing focused Gaussian laser beams. We used a two-photon excitation in a three-level system of Na_2 molecules by counterpropagating laser beams, which enabled us to exclude Doppler broadening such that the transit time effect is the dominant broadening mechanism. The conclusions drawn in this paper are generally applicable also to the case of one-photon excitation, given that Doppler broadening is not dominant.

We have shown that the interplay between two effects known to affect line broadening upon the interaction of molecules with tightly focused Gaussian laser beams, the curvature of electromagnetic field wave fronts and the increasing transit time of molecules with increasing distance z from the laser beam waist, counteract each other. The net effect is that only one parameter, the waist size of the laser beam, determines the transit time broadening. If the natural lifetime is comparable to transit time, then the resultant excitation line is described by a Voigt-like profile, a circumstance that should be taken into account in order to correctly estimate both the form and the width of lines in the excitation spectra.

We have demonstrated that for sufficiently large one-photon detunings and sufficiently low effective Rabi frequencies the effects of transit time in a two-photon excitation can be well described using a simple analytical two-level model. We have also defined the range of parameters within which the two-level model can be applied. The two-level model is validated by comparing its results with those of accurate numerical simulations using the density-matrix equations of motion and split-propagation technique. The numerical simulations also show that the distribution of transit times through the laser beams due to finite thermal velocity distribution of molecules in the beam can be disregarded for the typical supersonic beam conditions, when velocity dispersion of particles in the beam is low compared to the mean flow velocity (in our experiment the respective ratio is $\approx 1 : 5$). Note that the description provided in this paper is not valid for diffusive atomic and molecular beams as such distributions require a separate analysis due to their broad Maxwell velocity distributions.

ACKNOWLEDGMENTS

This work was carried out within the EU FP7 Centre of Excellence FOTONIKA-LV. Partial support by the EU FP7 IRSES Project COLIMA, a trilateral grant of Latvian,

Lithuanian, and Taiwanese Research Councils, and a grant from the President of the Russian Federation, Grant No. MK-3727.2011.2 (D.T.), are acknowledged. We thank A. Svarcs

for technical assistance, A. Markovski for programming assistance, and K. Bergmann, B. Shore, and M. Auzinsh for helpful discussions.

-
- [1] F. Biraben, M. Bassini, and B. Cagnac, *J. Phys. (Paris)* **40**, 445 (1979).
- [2] J. E. Thomas and W. W. Quivers, *Phys. Rev. A* **22**, 2115 (1980).
- [3] J. E. Thomas, M. J. Kelly, J. P. Monchalin, N. A. Kurnit, and A. Javan, *Phys. Rev. A* **15**, 2356 (1977).
- [4] W. Gawlik, *Phys. Rev. A* **34**, 3760 (1986).
- [5] G. Galzerano, E. Fasci, A. Castrillo, N. Coluccelli, L. Gianfrani, and P. Laporta, *Opt. Lett.* **34**, 3107 (2009).
- [6] W. Demtröder, in *Laser Spectroscopy* (Springer, Berlin, 2008), pp. 61–98.
- [7] J. E. Bjorkholm, P. F. Liao, and A. Wokaun, *Phys. Rev. A* **26**, 2643 (1982).
- [8] J. Ishikawa, F. Riehle, J. Helmcke, and C. J. Bordé, *Phys. Rev. A* **49**, 4794 (1994).
- [9] C. J. Bordé, J. L. Hall, C. V. Kunasz, and D. G. Hummer, *Phys. Rev. A* **14**, 236 (1976).
- [10] G. Moon and H.-R. Noh, *J. Opt. Soc. Am. B* **25**, 2101 (2008).
- [11] G. Moon and H.-R. Noh, *Opt. Commun.* **281**, 294 (2008).
- [12] G. Moon, H.-S. Noh, and H.-R. Noh, *J. Phys. Soc. Jpn.* **77**, 074301 (2008).
- [13] J. Hald, J. C. Petersen, and J. Henningsen, *Phys. Rev. Lett.* **98**, 213902 (2007).
- [14] J. L. Cohen and P. R. Berman, *Phys. Rev. A* **54**, 5262 (1996).
- [15] T. Wang, C. Greiner, J. R. Bochinski, and T. W. Mossberg, *Phys. Rev. A* **60**, R757 (1999).
- [16] M. A. Gubin and E. D. Protsenko, *Quantum Electron.* **27**, 1048 (1997).
- [17] C. J. Bordé, *Metrologia* **39**, 435 (2002).
- [18] J. L. Hall, *Rev. Mod. Phys.* **78**, 1279 (2006).
- [19] W. Ma, A. Foltynowicz, and O. Axner, *J. Opt. Soc. Am. B* **25**, 1144 (2008).
- [20] A. Foltynowicz, F. Schmidt, W. Ma, and O. Axner, *Appl. Phys. B* **92**, 313 (2008).
- [21] I. Sydoryk, N. N. Bezuglov, I. I. Beterov, K. Miculis, E. Saks, A. Janovs, P. Spels, and A. Ekers, *Phys. Rev. A* **77**, 042511 (2008).
- [22] M. Auzinsh, K. Bluss, R. Ferber, F. Gahbauer, A. Jarmola, M. S. Safronova, U. I. Safronova, and M. Tamanis, *Phys. Rev. A* **75**, 022502 (2007).
- [23] M. Auzinsh, R. Ferber, F. Gahbauer, A. Jarmola, and L. Kalvans, *Phys. Rev. A* **79**, 053404 (2009).
- [24] J. Sagle, R. K. Namiotka, and J. Huennekens, *J. Phys. B* **29**, 2629 (1996).
- [25] K. Shimoda, in *High-Resolution Laser Spectroscopy*, Topics in Applied Physics Vol. 13, edited by K. Shimoda (Springer, Berlin, 1976), pp. 11–49.
- [26] W. Demtröder, in *Atoms, Molecules and Photons*, Graduate Texts in Physics (Springer, Berlin, 2010), pp. 247–288.
- [27] C. Cohen-Tannoudji, J. Dupont-Roc, and G. Grynberg, in *Atom-Photon Interactions* (Wiley-VCH, Weinheim, Germany, 2008), pp. 353–405.
- [28] B. Shore, *The Theory of Coherent Atomic Excitation*, Vol. 2, *Multilevel Atoms and Incoherence* (Wiley, New York, 1990), p. 1736.
- [29] S. Stenholm, *Foundations of Laser Spectroscopy* (Dover, Mineola, NY, 2005).
- [30] M. G. Raymer and J. Cooper, *Phys. Rev. A* **20**, 2238 (1979).
- [31] N. Bezuglov, M. Zakharov, A. Klyucharev, A. Matveev, K. Michulis, E. Saks, I. Sydoryk, and A. Ekers, *Opt. Spectrosc.* **102**, 819 (2007).
- [32] G. Scoles, *Atomic and Molecular Beam Methods*, edited by G. Scoles, D. Bassi, U. Buck, and D. Lainé (Oxford University Press, Oxford, 1988), Vol. 1.
- [33] K. Bergmann, U. Hefter, and P. Hering, *Chem. Phys.* **32**, 329 (1978).
- [34] N. N. Bezuglov, A. Ekers, O. Kaufmann, K. Bergmann, F. Fuso, and M. Allegrini, *J. Chem. Phys.* **119**, 7094 (2003).
- [35] G. Baumgartner, H. Kornmeier, and W. Preuss, *Chem. Phys. Lett.* **107**, 13 (1984).
- [36] N. N. Bezuglov, R. Garcia-Fernandez, A. Ekers, K. Miculis, L. P. Yatsenko, and K. Bergmann, *Phys. Rev. A* **78**, 053804 (2008).
- [37] S. H. Autler and C. H. Townes, *Phys. Rev.* **100**, 703 (1955).
- [38] R. Garcia-Fernandez, A. Ekers, J. Klavins, L. P. Yatsenko, N. N. Bezuglov, B. W. Shore, and K. Bergmann, *Phys. Rev. A* **71**, 023401 (2005).
- [39] C. Davis, *Lasers and Electro-optics: Fundamentals and Engineering* (Cambridge University Press, Cambridge, 1996), p. 720.
- [40] V. Ivanov, *Transfer of Radiation in Spectral Lines*, National Bureau of Standards Special Publication Vol. 385 (National Bureau of Standards, Washington, DC, 1973).
- [41] J. Olivero and R. Longbothum, *J. Quant. Spectrosc. Radiat. Transfer* **17**, 233 (1977).
- [42] C. N. Cohen-Tannoudji, *Rev. Mod. Phys.* **70**, 707 (1998).
- [43] L. P. Yatsenko, S. Guérin, T. Halfmann, K. Böhmer, B. W. Shore, and K. Bergmann, *Phys. Rev. A* **58**, 4683 (1998).
- [44] S.-I. Chu and D. A. Telnov, *Phys. Rep.* **390**, 1 (2004).
- [45] S. Guerin, H. Jauslin, R. Unanyan, and L. Yatsenko, *Opt. Express* **4**, 84 (1999).
- [46] N. Delone and V. Krainov, *Atoms in Strong Light Fields*, Springer Series in Chemical Physics Vol. 28 (Springer, Berlin, 1985).
- [47] M. Auzinsh, N. N. Bezuglov, and K. Miculis, *Phys. Rev. A* **78**, 053415 (2008).
- [48] M. Feit, J. Fleck, and A. Steiger, *J. Comput. Phys.* **47**, 412 (1982).
- [49] A. K. Kazansky, N. N. Bezuglov, A. F. Molisch, F. Fuso, and M. Allegrini, *Phys. Rev. A* **64**, 022719 (2001).
- [50] I. Schmidt, Ph.D. thesis, Universität Kaiserslautern, 1987.
- [51] M. Külz, M. Keil, A. Kortyna, B. Schellhaas, J. Hauck, K. Bergmann, W. Meyer, and D. Weyh, *Phys. Rev. A* **53**, 3324 (1996).